



VCU

Virginia Commonwealth University
VCU Scholars Compass

Electrical and Computer Engineering Publications

Dept. of Electrical and Computer Engineering

2009

Internal quantum efficiency of c-plane InGaN and m-plane InGaN on Si and GaN

X. Ni

Virginia Commonwealth University

J. Lee

Virginia Commonwealth University

M. Wu

Virginia Commonwealth University

See next page for additional authors

Follow this and additional works at: http://scholarscompass.vcu.edu/egre_pubs

 Part of the [Electrical and Computer Engineering Commons](#)

Ni, X., Lee, J., Wu, M., et al. Internal quantum efficiency of c-plane InGaN and m-plane InGaN on Si and GaN. *Applied Physics Letters*, 95, 101106 (2009). Copyright © 2009 AIP Publishing LLC.

Downloaded from

http://scholarscompass.vcu.edu/egre_pubs/83

This Article is brought to you for free and open access by the Dept. of Electrical and Computer Engineering at VCU Scholars Compass. It has been accepted for inclusion in Electrical and Computer Engineering Publications by an authorized administrator of VCU Scholars Compass. For more information, please contact libcompass@vcu.edu.

Authors

X. Ni, J. Lee, M. Wu, X. Li, Ryoko Shimada, Ü. Özgür, A. A. Baski, Hadis Morkoç, T. Paskova, G. Mulholland, and K. R. Evans

Internal quantum efficiency of *c*-plane InGaN and *m*-plane InGaN on Si and GaN

X. Ni,^{1,a)} J. Lee,¹ M. Wu,¹ X. Li,¹ R. Shimada,¹ Ü. Özgür,¹ A. A. Baski,¹ H. Morkoç,^{1,b)} T. Paskova,² G. Mulholland,² and K. R. Evans²

¹Department of Electrical and Computer Engineering, Virginia Commonwealth University, Richmond, Virginia 23284, USA

²Kyma Technologies, Inc., Raleigh, North Carolina 27617, USA

(Received 15 July 2009; accepted 18 August 2009; published online 8 September 2009)

We investigated internal quantum efficiency (IQE) of polar (0001) InGaN on *c*-sapphire, and ($\bar{1}\bar{1}00$) nonpolar *m*-plane InGaN on both *m*-plane GaN and specially patterned Si. The IQE values were extracted from the resonant photoluminescence intensity versus the excitation power. Data indicate that at comparable generated carrier concentrations the efficiency of the *m*-plane InGaN on patterned Si is approximately a factor of 2 higher than that of the highly optimized *c*-plane layer. At the highest laser excitation employed ($\sim 1.2 \times 10^{18} \text{ cm}^{-3}$), the IQE of *m*-plane InGaN double heterostructure on Si is approximately 65%. We believe that the *m*-plane would remain inherently advantageous, particularly at high electrical injection levels, even with respect to highly optimized *c*-plane varieties. The observations could be attributed to the lack of polarization induced field and the predicted increased optical matrix elements in *m*-plane orientation. © 2009 American Institute of Physics. [doi:10.1063/1.3224192]

In the *c*-oriented GaN films, the internal spontaneous and strain-induced piezoelectric polarizations produce a strong electric field. This in turn causes spatial separation of electron and hole wave functions in quantum wells (QWs) used in light emitting diodes (LEDs) and laser diodes (LDs), thereby reducing the quantum efficiency, particularly at low injection levels.^{1,2} It also causes a redshift in LEDs and makes the emission wavelength dependent on injection current, blueshifting with injection, unless very thin QWs are employed. By employing nonpolar orientations, namely, *m*-plane^{3,4} or *a*-plane GaN,^{5,6} this problem could be circumvented. In particular, *m*-plane GaN is well suited for optoelectronic applications in that it is predicted to have a lower valence band density of states, reduced valence band effective mass, and thus smaller acceptor binding energy, and larger optical matrix elements relative to its *c*-plane counterpart, thereby improving the performance of LEDs and LDs.⁷ The abovementioned reduced hole effective mass would also help to obtain higher hole concentrations,^{8,9} thereby increasing radiative recombination rate as well as making it easier for holes to better equally distribute themselves throughout the active region. In this regard, the use of nonpolar orientations would assuage carrier spillover and help in efficiency retention at high injection levels.

In addition to performance issues, cost is another factor that is important in the manufacture of device structures. Even the cost of sapphire is certain to become a point of concern. Use of more economical substrates such as Si can answer this concern if the quality is not compromised. It would be particularly beneficial if Si could be used to produce *m*-plane GaN. Up to this point, however, *m*-plane GaN and LEDs have been obtained on γ -LiAlO₂ (100),⁴ *a*-plane sapphire,^{10,11} *m*-plane SiC substrates,¹² and *m*-plane bulk GaN.^{9,13} So far no results have been reported about *m*-plane

nitrides or LEDs on Si substrates. In this letter, we present a comparative study of the internal quantum efficiency (IQE) of *c*-plane InGaN LED active layers grown on *c*-plane sapphire, *m*-plane InGaN LED active layer on specially patterned Si, as well as on bulk *m*-plane GaN determined by resonant optical excitation.

Four InGaN LED active layers were grown in a vertical low-pressure metalorganic chemical vapor deposition system. One pair of LED active layers incorporates 6 nm thick InGaN double heterostructure (DH) active regions and a second pair incorporates six period (InGaN:2 nm/In_{0.01}Ga_{0.99}N:3 nm) multiple quantum well (MQW) active regions. Each pair of LED active layers includes the following two orientations: *c*-plane on *c*-sapphire and *m*-plane on patterned Si (DH) or on freestanding *m*-plane GaN (MQW). All four samples have a 60 nm Si-doped In_{0.01}Ga_{0.99}N ($2 \times 10^{18} \text{ cm}^{-3}$) underlayer just beneath the active region for improved quality and are capped with a 100 nm thick GaN layer. The peak emission wavelength for the two *m*-plane LED active layers (In_{0.13}Ga_{0.87}N) is $\sim 395 \text{ nm}$, while that of the two *c*-plane LED active layers (In_{0.14}Ga_{0.86}N) is $\sim 410 \text{ nm}$. The radiative recombination efficiency is maximum for an In content leading to emission at about 405–410 nm,¹⁴ which means that wavelength not being the same in all layers would not favor the *m*-plane types. It should be mentioned that the In incorporation is highly substrate temperature dependent and appears to be orientation dependent as well, in agreement with previous observations. Although the substrate temperatures and other growth parameter were kept the same for *m*-plane and *c*-plane layers with the same type of active regions, lower emission peak wavelength in *m*-plane layers most probably resulted from lower In incorporation in *m*-plane compared to *c*-plane.

The *c*-plane GaN template on sapphire used for *c*-plane LED active layer growth has a threading dislocation density of $\sim 2 \times 10^8 \text{ cm}^{-2}$ and was grown with *in situ* SiN_x nanonetwork.¹⁵ The *m*-plane LED active layer on Si were

^{a)}Electronic mail: nix@vcu.edu.

^{b)}Electronic mail: hmorkoc@vcu.edu.

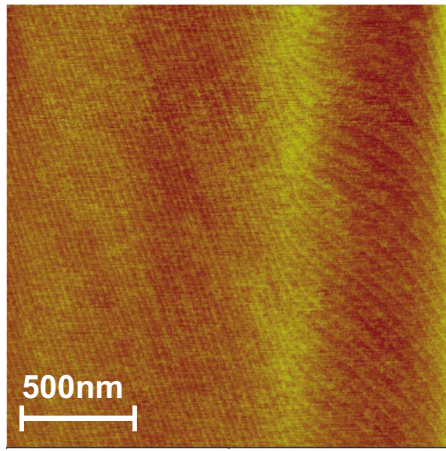


FIG. 1. (Color online) Tapping-mode AFM image ($\Delta z=10$ nm) of an *m*-plane GaN sample (~ 12 μm thick) grown on a patterned Si substrate. The AFM image indicates a very smooth surface (rms roughness of ~ 0.3 nm over an area of 2×2 μm^2) with clear atomic steps.

grown on *m*-plane GaN on a specially patterned Si substrate, the details of which will be presented at a later time. We should mention, however, growth of GaN on differently patterned Si has been reported previously.^{16–19} The *m*-plane freestanding GaN was provided by Kyma Technologies, and has a threading dislocations density of $< 5 \times 10^6$ cm^{-2} . Its off cut is 0.2° toward the GaN *a*-axis and 0.3° toward the GaN *c*-axis. Figure 1 shows an atomic force microscopy (AFM) image of the *m*-plane GaN on Si used for the *m*-plane InGaN LED active layer growth. The image indicates a very smooth surface (rms roughness of ~ 0.3 nm over an area of 2×2 μm^2) with clear atomic steps, suggesting a step-flow growth mode for this sample.

The photoluminescence (PL) studies with resonant excitation were carried out on the four LED active layer samples at room temperature using a frequency-doubled 80 MHz repetition rate femtosecond Ti:Sapphire laser. The excitation laser wavelength was 370 nm, below the bandgap of the quantum barriers and top GaN. As such, the photoexcited electron-hole pairs can only be generated within the QWs, thereby avoiding optical carrier generation in the barriers and also carrier injection effect, which has been observed to cause efficiency droop in the electroluminescence case.²⁰ During PL measurements, the average excitation power density was varied from 7 to 280 W/cm^2 using neutral density filters.

In order to measure the IQE with the resonant excitation PL, a method similar to the one described in Ref. 21 has been used. In our model we assume that at steady state the total generation rate (G) is equal to the total recombination rate (R), which includes Shockley–Read–Hall nonradiative recombination (An), bimolecular radiative recombination (Bn^2), and Auger recombination (Cn^3) if any, where n is the carrier concentration. The measured PL intensity could be represented as $I_{\text{PL}} = \eta_c B n^2$, where I_{PL} is the integrated PL intensity, the collection factor η_c includes escape efficiency of photons as well as the collection efficiency of luminescence by the optics/detector, which is constant during a given measurement but different from measurement to measurement even though attempts are made to keep the collection geometry the same. This variability does not, however, affect the values of the efficiencies reported here.

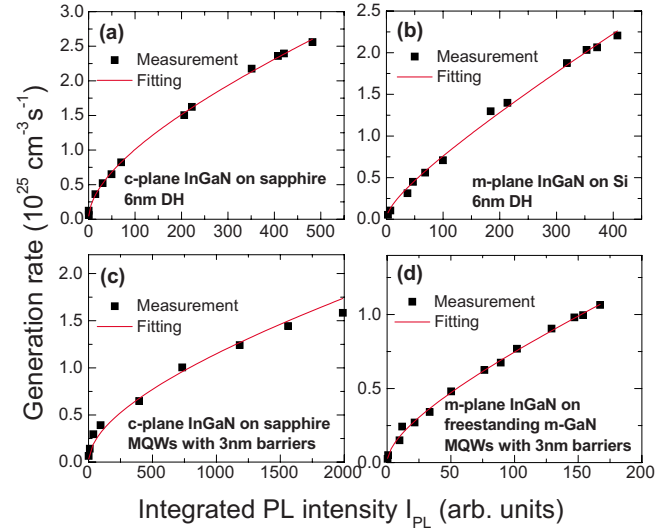


FIG. 2. (Color online) Curve fitting results of the generation rate as a function integrated PL intensity for (a) a *c*-plane LED active layer (with 6 nm InGaN DH) on sapphire and (b) an *m*-plane LED active layer (6 nm InGaN DH) on Si; Curve fittings for (c) a *c*-plane LED active layer on sapphire (MQWs structure with 3 nm InGaN barriers) and (d) an *m*-plane LED active layer on freestanding GaN (MQWs structure with 3 nm InGaN barriers). The red curves represent the fits obtained using Eq. (1).

From the above discussion it follows that the total generation rate at steady state is

$$G = \frac{A}{\sqrt{\eta_c B}} \sqrt{I_{\text{PL}}} + \frac{1}{\eta_c} I_{\text{PL}} + \frac{C}{(\eta_c B)^{3/2}} (\sqrt{I_{\text{PL}}})^{3/2}, \quad (1)$$

which can also be calculated separately from excitation laser power as described in Ref. 21 from $G = P_{\text{laser}}(1 - R)\alpha / (A_{\text{spot}} h\nu)$, where P_{laser} is the incident laser power, R is the Fresnel reflection coefficient, α is the absorption coefficient at the incident photon energy $h\nu$, and A_{spot} is the area of focused laser spot on the sample. By fitting the calculated generation rate as a function of the square root of integrated PL intensity $\sqrt{I_{\text{PL}}}$, the three coefficients for each term in Eq. (1) can be obtained, from which the $\text{IQE} = Bn^2/G = (I_{\text{PL}}/\eta_c)/G$ values are subsequently calculated. Knowing the B value, one can also obtain A and C recombination parameters. However, it should be mentioned here that the IQE does not depend on the assumed value of the B parameter (1×10^{-11} $\text{cm}^3 \text{s}^{-1}$ used here). Figure 2 shows the fitting of the generation rate as a function of the integrated PL intensity for all the LED active layer samples investigated here.

The extracted IQE values as a function of carrier concentration for all of the four LED active layer samples are summarized in Fig. 3. First, let us compare the *c*-plane LED active layer on sapphire and the *m*-plane LED active layer on Si, both of which have the same structure (6 nm thick InGaN active region) and were grown under the same conditions. At the same generated carrier concentrations IQE in the former LED active layer is approximately two times higher than that for the latter: 53% versus 28% at a carrier concentration of $\sim 8.5 \times 10^{17}$ cm^{-3} . At the highest laser excitation used (1.2×10^{18} cm^{-3}) the *m*-plane InGaN layer on Si has an IQE value of approximately 65%. Based on the extensive characterization of the template used for growth of the *c*-plane active layer structure, it is fair to assume that the active layer is of reasonable quality. We have also found out that IQE in

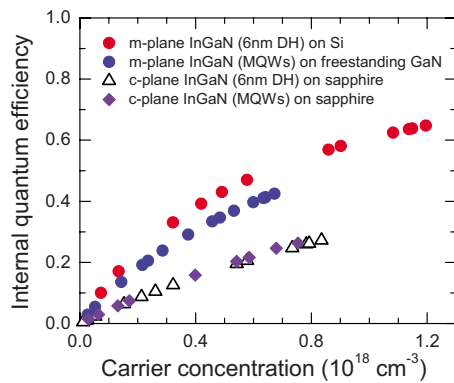


FIG. 3. (Color online) Extracted IQE values for the four LED active layers from the curve fittings. During the calculation of carrier concentrations for the four samples, the B coefficient was assumed to be $1 \times 10^{-11} \text{ cm}^3 \text{ s}^{-1}$.

c -plane LED active layers depends on the particulars of the active region such as the barrier height and barrier/QW thickness, with the measured values ranging from 20% to 50% in the carrier density range employed here. However, larger optical matrix elements for m -plane together with our preliminary data bode well for m -plane InGaN for light emitting devices, particularly those requiring large carrier injection.

Second, as shown in Fig. 3, at same carrier concentrations, the IQE values of the m -plane LED active layer on freestanding m -plane GaN are $\sim 70\%$ higher than those of its c -plane counterpart (42% and 25%, respectively, at a carrier concentration of $6.7 \times 10^{17} \text{ cm}^{-3}$), both of which have MQW active regions with 3 nm InGaN barriers. The above results suggest that m -plane LED active layers on both Si and freestanding m -GaN have an inherent advantage over their polar counterparts due to the elimination of polarization field, and thereby, enhanced electron-hole wave function overlap inside the active regions, and/or increased optical matrix elements.

Third, as a preliminary/rough comparison, the IQE values of the m -plane LED active layer on Si (6 nm thick InGaN DH) are slightly higher than those for the LED active layer grown on m -plane freestanding GaN (MQW structure with 3 nm InGaN barriers). This result is very promising in that comparable m -plane LED active layer (or even better) could be obtained on “inexpensive and abundantly available” Si substrates compared to “expensive” freestanding m -plane GaN.

To conclude, at the same carrier concentrations the IQE for m -plane LED active layer structures on specially patterned Si substrates is approximately two times higher than that for the c -plane LED active layer on sapphire with the same structure (a 6 nm thick InGaN double heterostructure). At the highest carrier density employed, the IQE in m -plane LED active layer on Si reaches approximately 65%, com-

pared to 28% for the c -plane LED active layer on sapphire. It is expected that the m -plane variety would outperform the c -plane variety in LEDs due to not only the absence of polarization field but also the relatively low hole mass (the latter would allow higher hole concentrations as well as better hole transport through the active region) and relatively large optical matrix elements, which would be extremely beneficial for reducing the nonthermal degradation of the LED efficiency with increasing injection levels.

The work at VCU is funded by the National Science Foundation (DMR, under Dr. Verne Hess). Partial support by ARO under Phase II W911NF-07-C-0099 contract for non-polar bulk development at Kyma Technologies, Inc., is acknowledged. Discussions with Dr. C. Tran of SemiLEDs on the general topic of nonpolar surfaces in conjunction with LEDs are appreciated.

- ¹R. Langer, J. Simon, V. Ortiz, N. T. Pelekanos, A. Barski, R. Andre, and M. Godlewski, *Appl. Phys. Lett.* **74**, 3827 (1999).
- ²T. Deguchi, K. Sekiguchi, A. Nakamura, T. Sota, R. Matsuo, S. Chichibu, and S. Nakamura, *Jpn. J. Appl. Phys., Part 2* **38**, L914 (1999).
- ³Y. J. Sun, O. Brandt, S. Cronenberg, S. Dhar, H. T. Grahn, K. H. Ploog, P. Waltereit, and J. S. Speck, *Phys. Rev. B* **67**, 041306 (2003).
- ⁴P. Waltereit, O. Brandt, A. Trampert, H. T. Grahn, J. Menniger, M. Ramsteiner, M. Reiche, and K. H. Ploog, *Nature (London)* **406**, 865 (2000).
- ⁵H. M. Ng, *Appl. Phys. Lett.* **80**, 4369 (2002).
- ⁶M. D. Craven, S. H. Lim, F. Wu, J. S. Speck, and S. P. DenBaars, *Appl. Phys. Lett.* **81**, 469 (2002).
- ⁷A. Niwa, T. Ohtoshi, and T. Kuroda, *Appl. Phys. Lett.* **70**, 2159 (1997).
- ⁸M. McLaurin, T. E. Mates, F. Wu, and J. S. Speck, *J. Appl. Phys.* **100**, 063707 (2006).
- ⁹M. McLaurin and J. S. Speck, *Phys. Status Solidi (RRL)* **1**, 110 (2007).
- ¹⁰K. Okuno, Y. Saito, S. Boyama, N. Nakada, S. Nitta, R. G. Tohmon, Y. Ushida, and N. Shibata, *Appl. Phys. Express* **2**, 031002 (2009).
- ¹¹Y. Saito, K. Okuno, S. Boyama, N. Nakada, S. Nitta, Y. Ushida, and N. Shibata, *Appl. Phys. Express* **2**, 041001 (2009).
- ¹²M. McLaurin, T. E. Mates, and J. S. Speck, *Appl. Phys. Lett.* **86**, 262104 (2005).
- ¹³K. C. Kim, M. C. Schmidt, H. Sato, F. Wu, N. Fellows, M. Saito, K. Fujito, J. S. Speck, S. Nakamura, and S. P. DenBaars, *Phys. Status Solidi (RRL)* **1**, 125 (2007).
- ¹⁴H. Morkoç, *Handbook of Nitride Semiconductors and Devices* (Wiley, Berlin, 2008), Vol. 3.
- ¹⁵J. Xie, Ü. Özgür, Y. Fu, X. Ni, H. Morkoç, C. K. Inoki, T. S. Kuan, J. V. Foreman, and H. O. Everitt, *Appl. Phys. Lett.* **90**, 041107 (2007).
- ¹⁶N. Sawaki, T. Hikosaka, N. Koide, S. Tanaka, Y. Honda, and M. Yamaguchi, *J. Cryst. Growth* **311**, 2867 (2009).
- ¹⁷Y. Honda, N. Kameshiro, M. Yamaguchi, and N. Sawaki, *J. Cryst. Growth* **242**, 82 (2002).
- ¹⁸K. Tomita, T. Hikosaka, T. Kachi, and N. Sawaki, *J. Cryst. Growth* **311**, 2883 (2009).
- ¹⁹T. Tanikawa, D. Rudolph, T. Hikosaka, Y. Honda, M. Yamaguchi, and N. Sawaki, *J. Cryst. Growth* **310**, 4999 (2008).
- ²⁰X. Ni, Q. Fan, R. Shimada, Ü. Özgür, and H. Morkoç, *Appl. Phys. Lett.* **93**, 171113 (2008).
- ²¹Q. Dai, M. F. Schubert, M. H. Kim, J. K. Kim, E. F. Schubert, D. D. Koleske, M. H. Crawford, S. R. Lee, A. J. Fischer, G. Thaler, and M. A. Banas, *Appl. Phys. Lett.* **94**, 111109 (2009).